


# Astrocyte lipid metabolism is critical for synapse development and function in vivo

Anne-Lieke F. van Deijk<sup>1</sup> | Nutabi Camargo<sup>1</sup> | Jaap Timmerman<sup>2</sup> | Tim Heistek<sup>2</sup> |  
Jos F. Brouwers<sup>3</sup> | Floriana Mogavero<sup>1</sup> | Huibert D. Mansvelder<sup>2</sup> |  
August B. Smit<sup>1</sup> | Mark H.G. Verheijen<sup>1</sup> 

<sup>1</sup>Department of Molecular & Cellular Neurobiology, Center for Neurogenomics and Cognitive Research, Amsterdam Neuroscience, VU University Amsterdam, De Boelelaan 1085, Amsterdam, 1081 HV, The Netherlands

<sup>2</sup>Department of Integrative Neurophysiology, Center for Neurogenomics and Cognitive Research, Amsterdam Neuroscience, VU University Amsterdam, De Boelelaan 1085, Amsterdam, 1081 HV, The Netherlands

<sup>3</sup>Department of Biochemistry and Cell Biology, Faculty of Veterinary Medicine, Yalelaan 1, 3584 CL Utrecht University, Utrecht, The Netherlands

## Correspondence

M.H.G. Verheijen, Department of Molecular & Cellular Neurobiology, Center for Neurogenomics and Cognitive Research, Amsterdam Neuroscience, VU University Amsterdam, De Boelelaan 1085, 1081 HV Amsterdam, The Netherlands.  
Email: mark.verheijen@vu.nl

## Abstract

The brain is considered to be autonomous in lipid synthesis with astrocytes producing lipids far more efficiently than neurons. Accordingly, it is generally assumed that astrocyte-derived lipids are taken up by neurons to support synapse formation and function. Initial confirmation of this assumption has been obtained in cell cultures, but whether astrocyte-derived lipids support synapses in vivo is not known. Here, we address this issue and determined the role of astrocyte lipid metabolism in hippocampal synapse formation and function in vivo. Hippocampal protein expression for the sterol regulatory element-binding protein (SREBP) and its target gene fatty acid synthase (*Fasn*) was found in astrocytes but not in neurons. Diminishing SREBP activity in astrocytes using mice in which the SREBP cleavage-activating protein (SCAP) was deleted from GFAP-expressing cells resulted in decreased cholesterol and phospholipid secretion by astrocytes. Interestingly, SCAP mutant mice showed more immature synapses, lower presynaptic protein SNAP-25 levels as well as reduced numbers of synaptic vesicles, indicating impaired development of the presynaptic terminal. Accordingly, hippocampal short-term and long-term synaptic plasticity were defective in mutant mice. These findings establish a critical role for astrocyte lipid metabolism in presynaptic terminal development and function in vivo.

## KEYWORDS

cholesterol, fatty acids, FASN, hippocampus, glia, interactions, plasticity, SCAP, SNAP-25, SREBP

## 1 | INTRODUCTION

Lipids are vital components of neuronal membranes and influence brain function in many different ways (Camargo, Smit, & Verheijen, 2009; Piomelli, Astarita, & Rapaka, 2007). Cholesterol and unsaturated fatty acids are enriched in the synaptic membrane, in which they are important determinants for a range of biochemical processes, for example, membrane fluidity, vesicle formation and fusion, ion channel function and the formation of specialized microdomains that contribute to cellular communication (Allen, Halverson-Tamboli, & Rasenick, 2007; Piomelli et al., 2007). Indeed, cholesterol is a major component of lipid rafts, and is proposed to be required presynaptically for synaptic vesicle formation (Thiele, Hannah, Fahrenholz, & Huttner, 2000), and postsynaptically for the clustering and stability of neurotransmitter receptors (Allen et al., 2007). Consequently, perturbed lipid metabolism affects

synaptic function (Hering, Lin, & Sheng, 2003; Jang, Park, & Kaang, 2009; Kotti, Head, McKenna, & Russell, 2008), which becomes apparent in several neurological disorders, for example, Niemann-Pick's disease (NPC), Alzheimer's disease (AD), Huntington's disease (HD), and Smith-Lemli-Opitz syndrome (Chen, Li, Chen, Gu, & Duan, 2007; Patel et al., 1999; Spell et al., 2004; Valenza et al., 2005; Waterham et al., 1998). Importantly, the brain is considered autonomous in lipid metabolism because of the blood-brain barrier that prevents lipids from entering the brain. Neurons themselves are inefficient in lipids synthesis and therefore rely on the uptake of lipids from the external environment (Dietschy & Turley, 2004; Nieweg, Schaller, & Pfrieger, 2009; Pfrieger & Ungerer, 2011). In vitro studies have demonstrated that astrocytes synthesize and release lipids that are complexed to apolipoprotein E (ApoE)-containing lipoproteins (Boyles, Pitas, Wilson, Mahley, & Taylor, 1985; Mauch et al., 2001; Medina & Tabernero, 2002;

Nieweg et al., 2009; Pfrieger & Ungerer, 2011). These lipoproteins can be taken up by neurons and thereby contribute to the formation, maturation and maintenance of synapses in vitro (Christopherson et al., 2005; Goritz et al., 2007; Mauch et al., 2001; Nagler, Mauch, & Pfrieger, 2001; Pfrieger, 2003b). Whereas these studies indicate a role for astrocyte-derived lipids in synapse development and function, in vivo evidence for this is lacking. Recently, we found that cholesterol and fatty acid synthesis in astrocytes relies on sterol regulatory element binding proteins (SREBPs; Camargo et al., 2012). SREBPs, consisting of SREBP-1a, SREBP-1c, and SREBP-2, belong to the family of basic helix-loop-helix leucine zipper (bHLH-Zip) transcription factors that govern the transcriptional activation of genes involved in fatty acid and cholesterol metabolism (Eberle, Hegarty, Bossard, Ferre, & Foufelle, 2004; Hua et al., 1993; Yokoyama et al., 1993). SREBP transcription factors crucially rely on post-translational activation involving the sterol sensor SREBP cleavage-activating protein (SCAP). Here, we used astrocyte-restricted inactivation of SCAP-SREBP-mediated lipid biogenesis to determine the role of astrocyte lipid metabolism in synapse formation and function in the hippocampus. We found that astrocytes are the predominant SREBP pathway-expressing cell type in the hippocampus, and that reduction of SREBP activity in astrocytes resulted in impaired presynaptic terminal function and synaptic plasticity, possibly via a decrease in the presynaptic protein SNAP-25 levels and the number of synaptic vesicles. Together, our data establish that astrocyte lipid metabolism is critical for proper presynaptic terminal development and hippocampal function in vivo.

## 2 | MATERIALS AND METHODS

### 2.1 | Animals

All experimental procedures were approved by the local animal research committee and complied with the European Council Directive (86/609/EEC). SCAP-floxed mice were obtained from the Jackson Laboratory and have been described previously (Matsuda et al., 2001). In addition, the hGFAP-Cre-IRES-LacZ transgenic mice have been described previously (Bajenaru et al., 2002). Both mouse lines were maintained on a C57Bl/6 background. In subsequent generations, we obtained mice with the genotype SCAP<sup>lox/lox</sup>, which are referred to as "SCAP mutants". Littermates with genotypes SCAP<sup>lox/wt</sup> or SCAP<sup>wt/wt</sup> are referred to as controls (Camargo et al., 2012). Mice of both sexes were used at the age of 2.5–3.5 month-old, unless indicated otherwise. Mice were housed with littermates of the same gender in Macrolon cages on sawdust bedding, after weaning (three weeks after birth), for the purpose of animal welfare. Food (Harlan Teklad, 2016) and water were provided ad libitum. Housing was controlled for temperature, humidity, and light-dark cycle (7 a.m. lights on, 7 p.m. lights off).

### 2.2 | Long-term plasticity measurements in hippocampal brain slices

Acute hippocampal coronal slices (400  $\mu$ m thick) were prepared from male SCAP mutant mice ( $n = 15$ ) or littermate controls ( $n = 20$ ). Slices

were cut in ice-cold slicing artificial cerebrospinal fluid (ACSF) containing the following (in mM): 125 NaCl, 3 KCl, 1.25 NaH<sub>2</sub>PO<sub>4</sub>, 26 NaHCO<sub>3</sub>, 10 glucose, 3 MgSO<sub>4</sub>, and 1 CaCl<sub>2</sub> (osmolarity 300 mOsm), and carboxygenated with 95%O<sub>2</sub>/5%CO<sub>2</sub>. Slices were allowed to recover for 1 hr at room temperature (RT) in modified carboxygenated ACSF containing (in mM): 125 NaCl, 3 KCl, 1.25 NaH<sub>2</sub>PO<sub>4</sub>, 26 NaHCO<sub>3</sub>, 10 glucose, 1 MgSO<sub>4</sub>, 3 CaCl<sub>2</sub>, and 0.01 glycine (osmolarity 300 mOsm). Slices were superfused with 1–2 ml/min carboxygenated ACSF at RT. Field excitatory postsynaptic potentials (fEPSPs) were induced by an extracellular stimulating electrode in the Schaffer collateral pathway, and were recorded with multiple electrodes in the dendritic layer of the CA1 neurons, using a planar 64-channel multi-electrode recording setup (MED64; Alpha MED Sciences). Based on the stimulus-response curve, a stimulation intensity was chosen that evoked a half-maximal fEPSP. After at least 10 min of stable baseline recording at 0.05 Hz, long-term potentiation (LTP) was induced by 1 s stimulation at 100 Hz (tetanus stimulation) repeated 4 times with 30 s interval. The fEPSPs were recorded for 1 hr after the tetanus. The amount of LTP is quantified as the change in average amplitude of the fEPSP taken of the 40–50 min interval following LTP induction.

### 2.3 | Short-term plasticity measurements

Horizontal hippocampal brain slices (300  $\mu$ m thick) were prepared from male control ( $n = 7$ ) and SCAP mutant mice ( $n = 6$ ). Slices were left for 1 hr to recover before recording. Slices were placed in a submerged recording chamber at 28–32°C and were superfused with ACSF. Whole-cell patch clamp recordings were made from pyramidal cells in the CA1 region under visual guidance by infrared differential interference contrast microscopy. Patch pipettes (3–5 megaohms) were pulled from standard-wall borosilicate tubing. Patch pipettes were filled with intracellular solution containing the following (in mM): 129 cesium gluconate; 1 CsCl; 10 HEPES; 4 K<sub>2</sub>-phosphocreatine; 10 tetraethylammonium; 4 ATP (magnesium salt); and 0.4 GTP (pH 7.2–7.3, pH adjusted with CsOH; osmolarity 290–300 mOsm). After the whole-cell configuration was established, the membrane potential was held at  $-70$  mV, and the internal solution was allowed to diffuse for 5 min into the cell prior to the onset of recording. The low intracellular chloride concentration in the pipette allowed a separation of excitatory and inhibitory synaptic events. Experiments in which inhibitory events occurred too close to the EPSCs measured were excluded from analysis.

Schaffer collateral fibers were stimulated using an extracellular electrode positioned in the stratum radiatum on the CA3 side. A stimulation intensity was used that evoked half-maximal EPSC amplitudes. Paired-pulse synaptic plasticity was induced by two pulses with a range of frequencies (2–50 Hz). For each frequency, the paired-pulse protocol was repeated 20 times, with a 15-s delay between each sweep. Sweeps at each frequency were measured in random order, allowing time-dependent changes in the responses to be identified. To assess significance, analysis of variance with repeated measures was used (for within subjects effect test, Huynh-Feldt was used after Mauchly's test for sphericity) as well as post hoc unpaired Student's *t*-test. Values  $\pm 2$  SD were removed from analysis.



## 2.4 | Golgi-cox staining

Mice ( $n = 3$  per genotype) were anesthetized with avertine and subjected to transcardiac perfusion with 0.1 M phosphate-buffered saline (PBS) followed by 4% paraformaldehyde (PFA) in 0.1 M PBS. For spine analyses, Golgi staining was conducted using the FD Rapid Golgi Stain Kit (FD Neurotechnologies), according to the manufacturer's guidelines. Brains were cryostat-sectioned at 100  $\mu\text{m}$ . Neurons were imaged using a Carl Zeiss LSM 510 meta scanner at 63 $\times$  magnification. Z-stacks were generated with Carl Zeiss LSM Image Browser 4.2 software. Z-stacks were analysed with ImageJ 1.47f software (NIH) for spine counting and spine head diameter. Spines were examined on dendrites of CA1 pyramidal neurons; 3–5 dendritic segments, each at least 10  $\mu\text{m}$  in length, were analyzed per neuron (ctrl:  $n = 31$ , mutant:  $n = 24$ ). Only spine heads that clearly protruded laterally from the dendritic shafts were counted. Spine density was calculated as number of spines per 10  $\mu\text{m}$  dendrite. Spine head diameter (of 17 neurons per genotype) was measured at the tip of the spine where the diameter was the largest (An et al., 2008; Meng et al., 2002).

## 2.5 | Electron microscopy

Excitatory synapses ( $n = 30$  per animal) of the hippocampal CA1 region of SCAP mutant mice ( $n = 3$ ) were compared with controls ( $n = 3$ ). Animals under deep anesthesia were subjected to transcardiac perfusion with 0.1 M PBS (pH 7.4) followed by freshly prepared cold PFA fixative (4% PFA, 2% glutaraldehyde in 0.1 M PBS, pH 7.4). Brains were removed and hippocampal sagittal sections of 50  $\mu\text{m}$  were postfixed in 1%  $\text{OsO}_4$  and stained with 1% ruthenium. After embedding in Epon, ultra-thin sections ( $\sim 90$  nm) containing the stratum radiatum were subsequently cut, collected on 400 mesh copper grids and stained with 1% uranyl acetate and lead citrate.

Digital images of asymmetric glutamatergic synapses were taken at 100,000 magnification using a Jeol 1010 (Peabody, MA) electron microscope. Only synapses with clear postsynaptic and presynaptic properties were selected for analysis. For each condition, docked vesicles, undocked vesicles, postsynaptic density (PSD) and active zone (AZ) length (nm), and vesicle cluster surface ( $\text{nm}^2$ ) were measured as described previously (Meijer et al., 2012), and depicted in Supporting Information Figure S1. Vesicles were characterized as docked when no separation was detectable between the vesicle membrane and the AZ. Cluster size is defined as the area within the presynaptic terminal that contains synaptic vesicles, both docked and undocked. Analysis was carried out blind to genotype.

## 2.6 | Immunohistochemistry

Animals ( $n = 3$  per genotype) were perfused transcardially with 0.1 M PBS followed by 4% PFA in 0.1 M PBS. Brains were removed, postfixed overnight at 4°C and cryoprotected with 30% sucrose in 0.1 M PBS for 4 days at 4°C. Brains were rapidly frozen in powdered dry ice and sliced into 40  $\mu\text{m}$ -thick sagittal sections on a cryostat. Free-floating sections containing the hippocampus were washed three times with 0.1 M PBS and blocked by incubation with blocking solution

(0.2% triton and 2.5% bovine serum albumin in 0.1 M PBS) for 1 hr followed by overnight incubation with primary antibodies in blocking solution at 4°C. The sections were rinsed four times in 0.1 M PBS and incubated in blocking solution containing the appropriate secondary antibody for 2 hr. Sections were rinsed four times with 0.1 M PBS and subsequently mounted in Vectashield mounting medium including DAPI as a nuclear dye (Vector Laboratories) on glass slides. The following primary antibodies were used mouse anti-GFAP (1:1,000, Sigma) and rabbit anti-FASN (1:1,000, Abcam). Secondary antibodies were Alexa fluor 568-conjugated goat anti-mouse and Alexa fluor 488-conjugated goat anti-rabbit.

## 2.7 | Hippocampal synaptosome preparation

Hippocampal synaptosomes were isolated from control and SCAP mutant mice ( $n = 6$  per genotype) as described previously (Klychnikov et al., 2010; Li et al., 2007). In brief, two hippocampi were pooled and homogenized in ice-cold homogenization buffer (0.32 M sucrose and 5 mM HEPES at pH 7.4) and centrifuged at 1000g for 10 min. Supernatant was loaded on top of a discontinuous sucrose gradient consisting of 0.85 and 1.2 M sucrose. After centrifugation for 2 hr at 110,000g, the synaptosomal fraction at the interface of 0.85 and 1.2 M sucrose was collected, rediluted in homogenisation buffer and the synaptosome fraction was resuspended in 150  $\mu\text{l}$  of 5 mM HEPES (pH 7.4) after centrifugation. Protein concentrations were determined using a Bradford assay (Bio-Rad). The obtained synaptosomes were used for immunoblotting analysis.

## 2.8 | Primary cell culture

Hippocampal astrocytes were collected from SCAP mutant mice or littermate controls (P1;  $n = 4$  per genotype). Genotyping was done on tails of the pups (at P1). Hippocampi were dissected, cleared of meninges and collected in ice-cold Hanks Buffered Salt Solution (HBSS; Sigma-Aldrich) buffered with 7 mM HEPES (pH 7.4; Invitrogen). The tissue was mechanically fragmented and incubated in HBSS, HEPES, and 0.25% trypsin (Invitrogen) at 37°C for 30 min. The trypsinization was quenched by adding Dulbecco's modified Eagle's medium (DMEM) + GlutaMAX (Gibco) supplemented with MEM nonessential amino acids solution (Sigma), 1% Pen/Strep (Invitrogen) and 10% fetal bovine serum (FBS; Gibco) and tissue was centrifuged at 1200 rpm for 10 min. The pellet was resuspended and cells were plated in poly-L-lysine (Gibco) coated T25 flasks (2 hippocampi from 1 pup per flask) for 7 days in DMEM supplemented with 10% FBS, and medium was changed every 2 days. After reaching confluence, cells were washed three times with PBS (pH 7.4; Invitrogen) and serum-free medium was added [neurobasal medium (Gibco) supplemented with N2 (Gibco)]. Astrocyte-conditioned medium (ACM) was harvested after 3 days of conditioning and analysed using mass spectrometry. Subsequently, astrocytes were prepared for immunoblotting.

Hippocampal neurons were collected from SCAP mutant mice or littermate controls (E18). Genotyping was done on tails of the embryos (at E18). Hippocampi were incubated in HBSS with HEPES and 0.25% trypsin at 37°C for 30 min. Tissue was washed twice with HBSS and HEPES

to remove trypsin. Subsequently, cells were dissociated by repeated trituration through a fire-polished Pasteur pipet, counted and plated in Neurobasal medium supplemented with B-27 (Gibco), 1.8% HEPEs, 5 mM glutamax (Invitrogen), and 0.1% Pen/Strep. Wells of 24-wells plates (Greiner) were pretreated with a mixture of poly-D-lysine (Sigma-Aldrich) and laminin (Sigma-Aldrich) overnight at 4°C. Subsequently, wells were washed and incubated with 5% horse serum (Gibco) for 2 hr at 37°C. Neurons from one animal were seeded in 4 wells at a density of 125K/well and cultures were maintained in 37°C/5% CO<sub>2</sub> for 14 days. Half of the medium was replaced at 2 and 9 days after plating.

## 2.9 | Mass spectrometry analysis of ACM

Lipids were isolated from three-day ACM by lipid extraction as described previously (Verheijen et al., 2009). Neutral lipids were analyzed by reverse phase HPLC-tandem mass spectroscopy on a Sciex 4000 Q-trap mass spectrometer (Sciex, Framingham, MA), equipped with an atmospheric pressure chemical ionization source. Intact phospholipids were analyzed by HILIC chromatography and mass spectrometry as described previously (Arroyo-Olarte et al., 2015). Levels of detected lipids in ACM were normalized to total protein content.

## 2.10 | Immunoblotting

### 2.10.1 | Immunoblotting of cultured cells

Primary cultures of astrocytes and neurons were briefly washed with PBS and harvested in SDS loading buffer and boiled for 5 min. Equal amounts of protein were loaded on SDS-PAGE in a Mini-Protein electrophoresis system (Bio-Rad Laboratories) and electroblotted overnight onto polyvinylidene difluoride membranes (PVDF, Bio-rad). Membranes were probed with SREBP1 primary antibody (gift from H. Shimano, University of Tsukuba, Tsukuba, Japan), followed by incubation with alkaline phosphatase-conjugated goat anti-rabbit secondary antibody (Dako, 1:10,000), followed by enhanced chemiluminescence femto (ECF) detection (Thermo Scientific). Membranes were scanned with the FLA instrument (Fujifilm) and protein expression was quantified using Quantity One software (Bio-Rad). To correct for input differences, the ECF signal was normalized to the total protein amount from each sample detected by 2,2,2-trichloroethanol (TCE) staining of the gel (Ladner, Yang, Turner, & Edwards, 2004).

### 2.10.2 | Immunoblotting of synaptosomes

Five microgram per synaptosome sample were dissolved in SDS loading buffer and heated to 90°C for 5 min. Proteins were separated on a SDS-polyacrylamide gel and electroblotted onto a PVDF membrane overnight at 40 V. Membranes were incubated with primary antibodies against postsynaptic proteins PSD-95 (Neuromab, 1:20,000), GluN1 (Neuromab, 1:1,000), GluN2A (Epitomics, 1:5,000), GluA1 (Abcam, 1:50,000), GluA2 (Neuromab, 1:2,000), mGluR2 (Abcam, 1:2,000), and presynaptic proteins Munc18 (1:1,000, gift from M. Verhage, VU University Amsterdam, The Netherlands), synaptotagmin (Hybrodoma, 1:1,000), synaptophysin (Genscript, 1:1,000), syntaxin (Genscript, 1:500), synaptobrevin (SySy, 1:5,000), and SNAP-25 (Sternberger,

1:10,000). Subsequently, the membranes were incubated with alkaline phosphatase-conjugated goat anti-mouse or goat anti-rabbit secondary antibody (Dako, 1:10,000). Immunodetection was performed using ECF (Thermo Scientific) according to the manufacturer's instructions. To correct for input differences, the ECF signal was normalized to the total protein amount from each sample detected by TCE staining of the gel (Ladner et al., 2004). Values  $\pm$  2 SD were removed from analysis.

## 2.11 | Statistical analysis

Statistical differences between SCAP mutant and control mice were analyzed using Student's *t*-test, unless otherwise indicated in the legends. Statistical numeric data are provided in the text (Results). Data are presented as mean  $\pm$  SEM.

# 3 | RESULTS

## 3.1 | GFAP-SCAP astrocytes are impaired in lipid synthesis and secretion

To determine the role of astrocyte-derived extracellular lipids in synapse formation and function, we first measured SREBP expression in neurons and astrocytes isolated from mutant GFAP-SCAP mice and littermate controls. This GFAP-Cre transgenic mouse line has been described to predominantly target Cre-mediated recombination in the majority of astrocytes (Bajenaru et al., 2002), and is notably very different from the extensively characterized hGFAP-Cre mouse that is used to target radial glia (Malatesta, Hack, Hartfuss, Kettenmann, Klinkert, Kirchhoff, & Gotz, 2003; Zhuo et al., 2001). Western blotting detected strong SREBP1 expression in control astrocytes, whereas no SREBP1 protein was detected in control neurons (Figure 1A). These findings are in line with previous studies showing that the level of lipid synthesis in hippocampal neurons is very low when compared with astrocytes (Chen, Zhang, Kusumo, Costa, & Guizzetti, 2013; Nieweg et al., 2009; Pfrieger & Ungerer, 2011). SREBP levels in astrocytes were strongly decreased in SCAP mutants when compared with controls (Figure 1A). In line with these measurements *in vitro*, hippocampal astrocytes, unlike neurons in the stratum pyramidale, express fatty acid synthase (FASN), a SREBP target gene (Figure 2). Astrocyte expression of FASN was high during early postnatal development (P14, Figure 2A-C), at lower levels in adults (P90, Figure 2G-I), and strongly reduced in SCAP mutants (Figure 2D-F, J-L). These data extend our previous transcriptional data (Camargo et al., 2012) and show that also protein levels of SREBPs and their target genes are strongly reduced in SCAP mutant astrocytes. Next, we determined whether lipid secretion by astrocytes is hampered by SCAP deletion. Mass spectrometry analysis of all lipids in astrocyte-conditioned medium (ACM) revealed that astrocytes secreted cholesterol, phosphatidylcholine (PC) and sphingomyelin (SM; Figure 1B), while other phospholipids, such as phosphatidylethanolamine (PE) or -inositol (PI), or -serine (PS) were present at trace levels only and contributed <1% to the total phospholipid content of the medium. SCAP mutant astrocytes secreted significantly less cholesterol (ctrl:  $18.25 \pm 1.82$  nmol/ml, *n* = 4; mt:  $5.89 \pm 2.12$  nmol/ml,

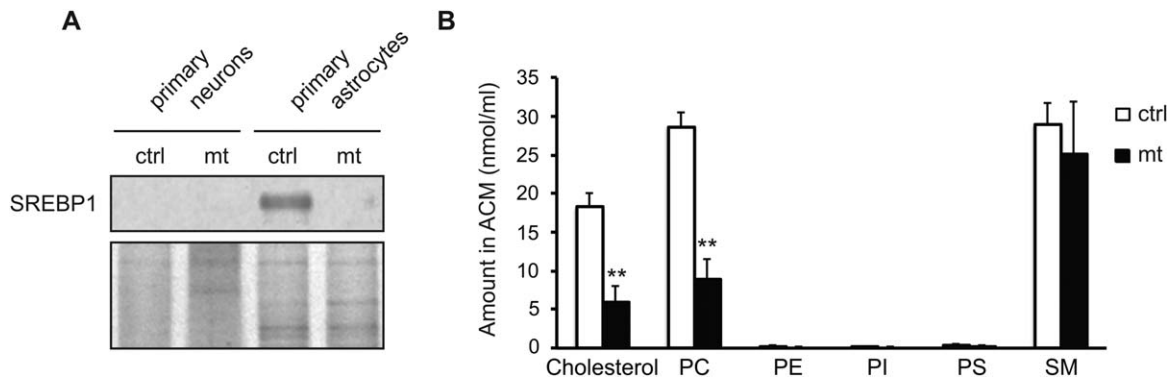


**FIGURE 1** SCAP gene deletion in astrocytes downregulates SREBP1 and lipid secretion. (A) Protein levels of precursor SREBP1 in primary cultures of neurons and astrocytes isolated from SCAP mutants (mt) and control (ctrl) littermates. Lower panel, in-gel protein stain to control for amount of protein loaded. (B) Quantification of lipids secreted by either ctrl or mt astrocytes cultured in serum-free medium ( $n = 4$  independent cultures from different animals), corrected for equal protein loading. ACM, astrocyte conditioned medium; PC, phosphatidylcholine; PE, phosphatidylethanolamine; PI, phosphatidylinositol; PS, phosphatidylserine; SM, sphingomyelin. Data are presented as mean  $\pm$  SEM. \*\* $p < .01$  using Student's  $t$ -test

$n = 4$ ;  $t(6) = 4.42$ ,  $p = .004$ ) and PC (ctrl:  $28.65 \pm 1.90$  nmol/ml,  $n = 4$ ; mt:  $8.93 \pm 2.65$  nmol/ml,  $n = 4$ ;  $t(6) = 6.05$ ,  $p = .001$ ), while secreted SM levels were unchanged (Figure 1B; ctrl:  $28.91 \pm 2.85$  nmol/ml,  $n = 4$ ; mt:  $25.11 \pm 6.89$  nmol/ml,  $n = 4$ ;  $t(6) = 0.51$ ,  $p = .63$ ). The latter is in line with SREBPs not being a transcriptional regulator of the sphingolipid synthetic enzyme (Worgall, 2011). Because cholesterol and PC are the main lipid components carried by lipoproteins, and form the major lipid efflux machinery of astrocytes (LaDu et al., 1998), SCAP deletion in astrocytes results in a major impairment of the synthesis and secretion of lipids.

### 3.2 | Astrocyte SCAP deletion causes impaired hippocampal spine maturation in vivo

The hippocampus of SCAP mutant mice is modestly reduced in total area, although without obvious morphological changes in specific layers or regions, and without obvious changes in cell numbers and morphology for neurons and astrocytes (Camargo et al., 2012). To examine whether SCAP mutant mice show changes in synapse number and morphology, Golgi-Cox analysis was performed on spines in the CA1 region of the hippocampus (Figure 3A). Hippocampal pyramidal neurons in SCAP mutant mice were found to exhibit a higher synapse density compared to controls (Figure 3B; ctrl:  $10.74 \pm 0.20$  spines/10  $\mu$ m dendrite,  $n = 31$ ; mt:  $11.69 \pm 0.32$  spines/10  $\mu$ m dendrite,  $n = 24$ ;  $t(53) = -2.62$ ,  $p = .012$ ). Spine head diameter in SCAP mutants was smaller (Figure 3C; ctrl:  $0.37 \pm 0.005$   $\mu$ m,  $n = 17$ ; mt:  $0.30 \pm 0.006$   $\mu$ m,  $n = 17$ ;  $t(32) = 8.24$ ,  $p = .000$ , Figure 3D), indicating that SCAP deletion in astrocytes leads to impaired hippocampal spine maturation, resulting in a high number of synapses that are immature.

### 3.3 | Astrocyte SCAP deletion causes changes in hippocampal synaptic protein expression

Next, we analyzed synaptic protein expression in hippocampal synaptosomes. No changes were found in the levels of postsynaptic

protein PSD-95 between control and SCAP mutant mice ( $n = 6$ , Figure 4A-B, Figure S1). Furthermore, no difference in protein levels of  $\alpha$ -amino-3-hydroxy-5-methyl-4-isoxazolepropionic acid receptor subunits (GluA1 and GluA2),  $N$ -Methyl-D-aspartic acid receptor subunits (GluN1 and GluN2A) or metabotropic glutamate receptor 2 (mGluR2) was found (Figure 4A-B, Figure S1). Thus, postsynaptic protein levels in the hippocampus of SCAP mutants appeared normal.

In contrast, analysis of presynaptic proteins revealed a significantly decreased level of synaptosomal-associated protein 25 (SNAP-25; ctrl:  $100 \pm 5.95$ ,  $n = 6$ ; mt:  $82.21 \pm 2.21$ ,  $n = 6$ ;  $t(8) = 2.80$ ,  $p = .023$ ) in SCAP whereas no significant changes were found for synaptotagmin (Synt), munc18 (M18), syntaxin1a (Stx1a), synaptophysin (Syn), and synaptobrevin2 (VAMP2; Figure 4C-D, Figure S2). Together, these results show that SCAP mutants have a specific reduction in the hippocampal presynaptic protein SNAP-25.

### 3.4 | Astrocyte SCAP deletion decreases the number of presynaptic docked vesicles

To examine whether dysregulation of presynaptic protein expression is correlated with subcellular changes of synapses, we performed ultrastructural analysis of excitatory/asymmetric synapses in the hippocampal region CA1 using electron microscopy (Figures 5A-D). Postsynaptic density (PSD) length was found unaffected (Figure 5B; ctrl:  $308.64 \pm 9.02$   $\mu$ m,  $n = 90$ ; mt:  $307.52 \pm 10.03$   $\mu$ m,  $n = 90$ ;  $t(178) = 0.08$ ,  $p = .934$ ), in line with our finding that SCAP mutants have normal PSD-95 protein levels in hippocampal synapses (Figure 4). Similarly, no difference in the size of the active zone (AZ) of the presynaptic terminal was found (Figure 5B; ctrl:  $285.08 \pm 8.07$   $\mu$ m,  $n = 90$ ; mt:  $303.06 \pm 10.39$   $\mu$ m,  $n = 90$ ;  $t(178) = -1.37$ ,  $p = .173$ ). However, quantitative analysis of synaptic vesicles revealed a significant decrease in the number of docked vesicles (Figure 5C; ctrl:  $3.89 \pm 0.14$ ,  $n = 90$ ; mt:  $3.19 \pm 0.17$ ,  $n = 90$ ;  $t(178) = 3.10$ ,  $p = .002$ ). Additionally, a trend was found towards a decrease in the number of undocked vesicles (Figure 5C;

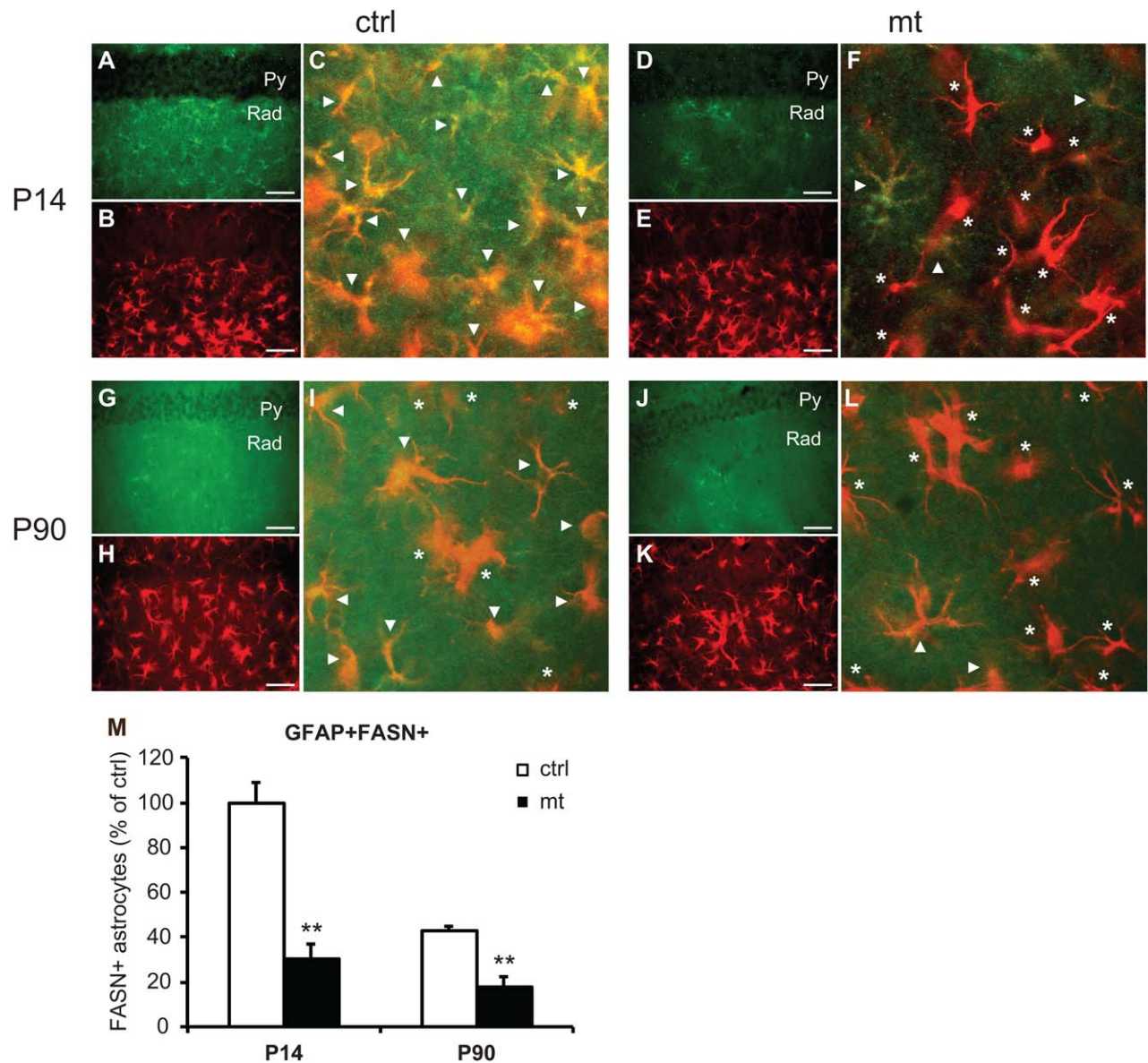


**FIGURE 2** FASN is expressed in astrocytes in the hippocampal region CA1, whereas expression is impaired in SCAP mutants. Expression of FASN (in green) in astrocytes (GFAP, in red) of (A–C) control or (D–F) SCAP mutant mice at P14, or of (G–I) control, or (J–L) SCAP mutant mice at P90. Arrowheads and asterisks denote astrocytes, respectively, with or without FASN expression. Neurons in the stratum pyramidale (Py) show no FASN expression. Rad, stratum radiatum. (M) Density of FASN-positive astrocytes (GFAP + FASN+) in control (ctrl) and mutant (mt) mice at p14 and P90. The values were normalized to P14 ctrl levels, which were set at 100%. Data are presented as mean  $\pm$  SEM. \*\* =  $p < .01$  using Student's *t*-test

ctrl:  $55.39 \pm 2.88$ ,  $n = 90$ ; mt:  $48.11 \pm 2.44$ ,  $n = 90$ ;  $t(178) = 1.93$ ,  $p = .056$ ). Accordingly, the total number of vesicles (ctrl:  $59.28 \pm 2.92$ ,  $n = 90$ ; mt:  $51.30 \pm 2.50$ ,  $n = 90$ ;  $t(178) = 2.08$ ,  $p = .039$ ) and the size of the vesicle cluster (ctrl:  $0.144 \pm 0.007 \mu\text{m}^2$ ,  $n = 90$ ; mt:  $0.121 \pm 0.006 \mu\text{m}^2$ ,  $n = 90$ ;  $t(178) = 2.39$ ,  $p = .018$ ) for mutant animals were significantly reduced (Figures 5C, E), as well as the number of docked vesicles per AZ length (Figure 5D; ctrl:  $100 \pm 3.54$ ,  $n = 90$ ; mt:  $75.42 \pm 3.37$ ,  $n = 90$ ;  $t(178) = 5.03$ ,  $p = .000$ ). Taken together, these data show that synapses of SCAP mutant mice have a compromised presynaptic terminal.

### 3.5 | Short-term plasticity is affected in SCAP mutants

Our biochemical and ultrastructural studies show that in particular presynaptic terminals of SCAP mutants are affected. To assess whether also presynaptic function is compromised, short-term synaptic plasticity was measured in the Schaffer collaterals of the hippocampus. Paired-pulse facilitation (PPF) or depression has been associated with presynaptic release properties (Abbott & Regehr, 2004) and change in presynaptic function can result in altered PPF or depression. PPF of excitatory synaptic transmission was observed in control mice at inter-stimulus intervals (ISI) 20–200 ms. Interestingly, PPF was significantly

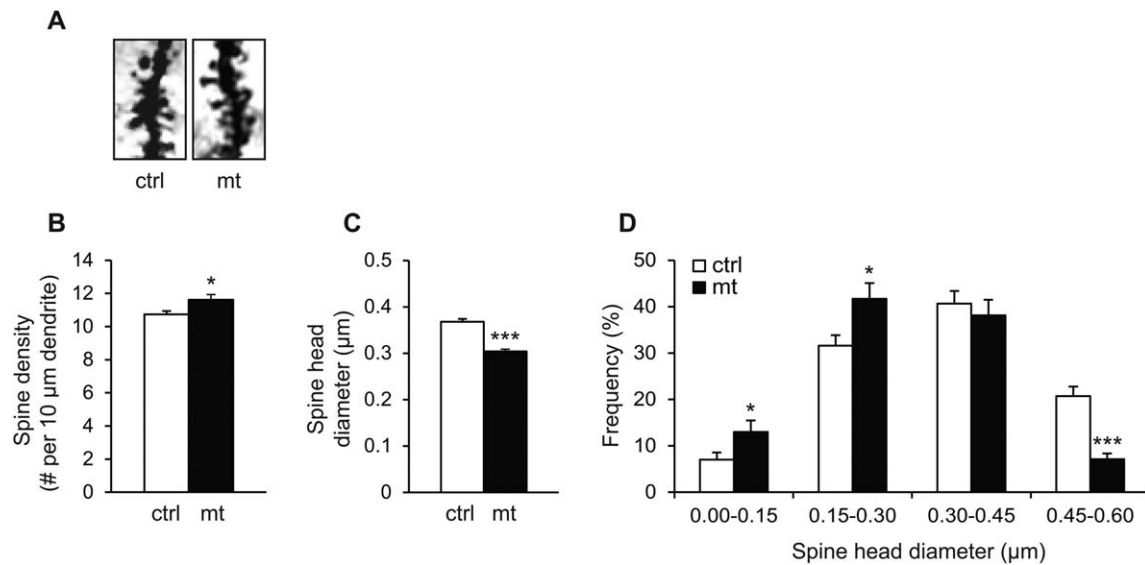


**FIGURE 3** SCAP gene deletion yields immature spines on hippocampal CA1 pyramidal neurons. (A) Representative images of dendritic segments of hippocampal CA1 pyramidal neurons of control (ctrl) and SCAP mutant (mt) mice. (B) Mean spine density of ctrl and mt animals, that is, the number of spines per 10  $\mu$ m dendritic segment.  $N = 31$  ctrl,  $n = 24$  mt cells. (C) Mean spine head diameter of ctrl and mt animals.  $N = 17$  cells per genotype. (D) Frequency distribution of spine head diameter.  $*p < .05$ ,  $***p < .001$ , using Student's  $t$ -test

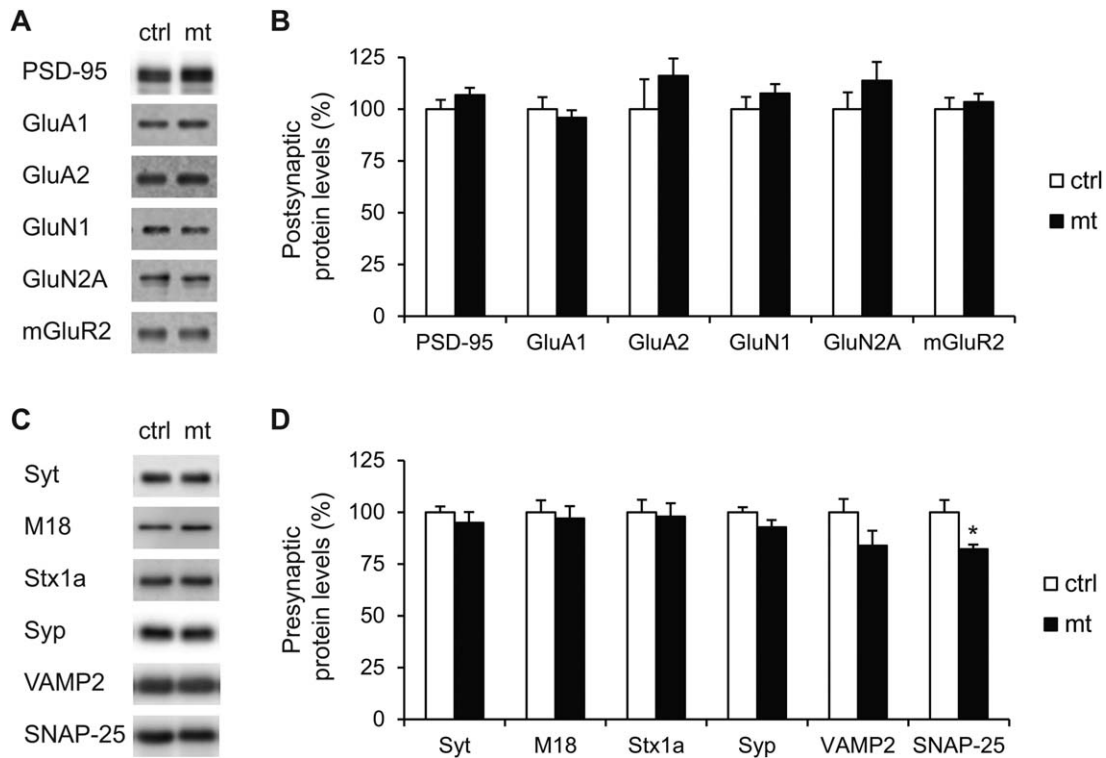


**FIGURE 4** SNAP-25 levels are reduced in hippocampal synaptosomes of SCAP mutant animals. (A, C) Representative blots of (A) postsynaptic and (C) presynaptic synaptic proteins detected in hippocampal synaptosomes using immuno-blotting. See Supporting Information Figure S1 and S2 for complete blots and for in-gel protein stain used to correct for equal protein loading. (B) Quantification of PSD-95 protein and glutamate receptors of control (ctrl) and SCAP mutant animals (mt;  $n = 6$  each). Bars represent protein levels after correction for equal loading using in-gel protein stain and subsequent normalization by setting ctrl levels at 100%. (D) Quantification of presynaptic proteins of ctrl and mt animals ( $n = 6$  each). To identify changes of presynaptic protein levels compared to postsynaptic protein levels, the presynaptic protein levels were corrected for PSD-95 level for each animal separately and subsequently normalized to ctrl levels by setting it to 100%. Syt, synaptotagmin; M18, munc18; Stx1a, syntaxin1a; syp, synaptophysin; VAMP2, vesicle-associated membrane protein 2 (synaptobrevin 2); SNAP-25, synaptosomal-associated protein 25. Data are presented as mean  $\pm$  SEM.  $*p < .05$ , Student's  $t$ -test

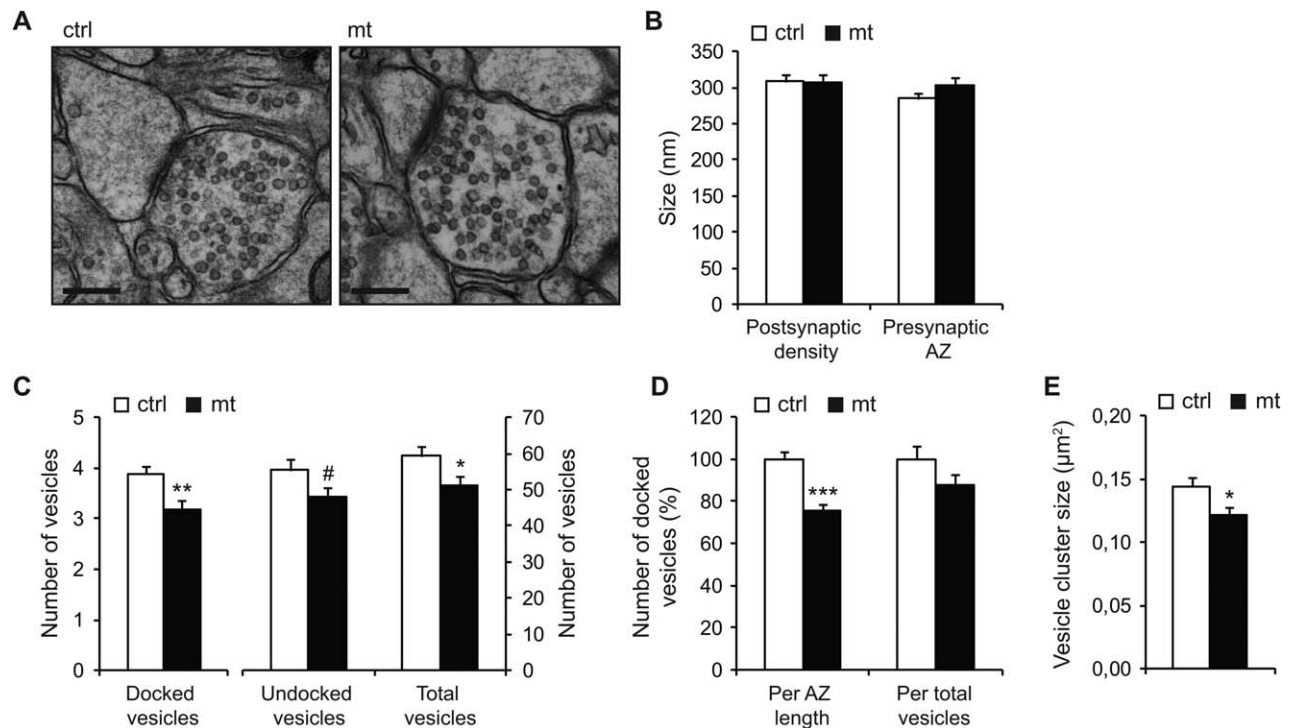


**FIGURE 5** CA1 asymmetric (excitatory) synapses in the stratum radiatum of SCAP mutant mice exhibit fewer vesicles. (A) Example of electron micrographs from asymmetric synapses of control (ctrl;  $n = 3$ ) and SCAP mutant (mt;  $n = 3$ ) animals. Scale bar equals 200 nm. See Supporting Information Figure S1 for explanation of quantified parameters. (B) Size of PSD and presynaptic AZ length of asymmetric synapses in ctrl and mt. (C) The number of docked vesicles (vesicles in direct contact to the AZ), undocked and total vesicles in ctrl and mt. (D) Number of docked vesicles per length of AZ (left) and number of docked vesicles to total number of vesicles (right) in ctrl and mt. Values are normalized to ctrl levels in which the ctrl levels are set to 100%. (E) Size of vesicle cluster in  $\mu\text{m}^2$ . Data are presented as mean of synapses per genotype ( $n = 90$ )  $\pm$  SEM. \* $p < .05$ , \*\* $p < .01$ , \*\*\* $p < .001$ , # $p = .056$ , Student's  $t$ -test

lower in SCAP mutant mice compared with control at ISI 20 ms (Figure 6C; ctrl:  $1.36 \pm 0.09$ ,  $n = 15$ ; mt:  $1.09 \pm 0.07$ ,  $n = 12$ ;  $t(25) = 2.29$ ,  $p = .031$ ), 50 ms (Figure 6C; ctrl:  $1.20 \pm 0.06$ ,  $n = 17$ ; mt:  $1.00 \pm 0.07$ ,  $n = 12$ ;  $t(27) = 2.19$ ,  $p = .037$ ), and 100 ms (Figures 6A–C; ctrl:  $1.13 \pm 0.05$ ,  $n = 18$ ; mt:  $0.92 \pm 0.04$ ,  $n = 15$ ;  $t(31) = 3.26$ ,  $p = .003$ ). These results show that short-term plasticity of hippocampal synapses in SCAP mutants is compromised and this most likely results from altered presynaptic release properties.

### 3.6 | SCAP mutants have reduced hippocampal long-term synaptic plasticity

To determine whether SCAP mutants have affected hippocampal long-term synaptic plasticity, we measured LTP in CA1, resulting from local field excitatory post-synaptic potentials (fEPSPs) at Schaffer collaterals from CA3 to CA1. Tetanic stimulation resulted in a potentiated synaptic response in controls, which was strongly impaired in SCAP mutants (Figures 7A–B; ctrl:  $126.01 \pm 4.43$ ,  $n = 20$ ; mt:  $106.07 \pm 3.89$ ,  $n = 15$ ;  $t(33) = 3.25$ ,  $p = .003$ ), showing that long-term synaptic plasticity is strongly affected at hippocampal synapses of SCAP mutant mice.

## 4 | DISCUSSION

In this study, we found that deletion of SREBP activity in astrocytes resulted in impaired presynaptic terminal function and synaptic plastic-

ity, possibly via a decrease in the presynaptic protein SNAP-25 levels and the number of synaptic vesicles. Our data establish that astrocyte lipid metabolism is critical for proper presynaptic terminal development and hippocampal function in vivo, which may have important implications for the understanding and treatment of neurological disorders that are associated with compromised brain lipid metabolism.

### 4.1 | Astrocyte SCAP deletion reduces cholesterol and PC secretion

Since neurons are much less active in lipid synthesis than astrocytes (Chen et al., 2013; Nieweg et al., 2009; Pfriger & Ungerer, 2011), they rely on lipids from external sources, which are presumably internalized by lipoprotein receptors located on the neuronal cell surface (Bu, Maksymovitch, Nerbonne, & Schwartz, 1994; Pfriger, 2003a). In line with this, we could not detect SREBP protein and FASN protein (transcriptionally regulated by SREBP) in hippocampal neurons, in contrast to astrocytes. In addition, astrocytes were highly active in the secretion of specifically cholesterol and PC, both cargo of lipoproteins (LaDu et al., 1998). Moreover, we extend our previous observations on GFAP-SCAP astrocytes (Camargo et al., 2012) and show that synthesis and secretion of lipids is impaired in astrocytes derived from GFAP-SCAP mutants. Taken together, this indicates that in GFAP-SCAP mice astrocyte lipid synthesis is highly compromised.

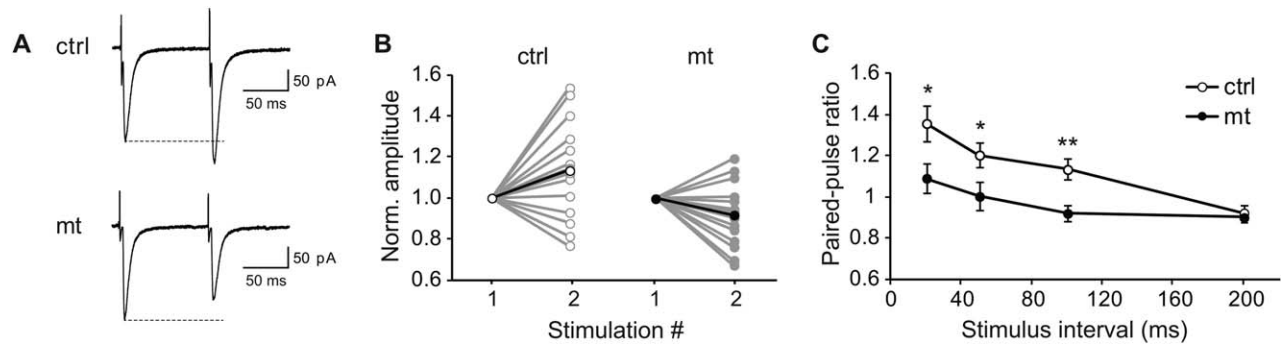


**FIGURE 6** SCAP mutants have impaired short-term plasticity (PPF) in the CA1 region of the hippocampus. (A) Representative EPSP trace of control (ctrl) and SCAP mutant (mt) pyramidal cells in hippocampal slices at 100 ms ISI. (B) Normalized amplitudes of pulse 2 over 1 (first signal is normalized to 1). Each pair of points (connected by gray lines) shows the averaged first and second EPSCs from individual experiments (mean of 20 stimulus trains). Points connected by a thick black line show the genotype averages. (C) Plot of PPR measured at different ISI (20–200 ms). Ratio between second and first signal is plotted against the ISI. Each point shows the mean of  $n = 13$ –18 measurements per ISI (each ISI consisting of 20 stimulus trains)  $\pm$  SEM,  $*p < .05$ ,  $**p < .01$

#### 4.2 | SCAP mutants have compromised synapse structure

We show that astrocyte lipogenic gene expression is high during early postnatal life (P14) whereas being low in adults (P90), which coincides with the period of synaptogenesis that peaks in the second postnatal week (Semple, Blomgren, Gimlin, Ferriero, & Noble-Haesslein, 2013). We found that compromised astrocyte lipid synthesis in SCAP mutants resulted in an increase in the number of synapses and smaller spine head diameters in the CA1 region of the hippocampus, indicating a larger number of more immature synapses (Harris & Stevens, 1989; Konur, Rabinowitz, Fenstermaker, & Yuste, 2003; Toni et al., 2007; Yuste & Bonhoeffer, 2004). The observations on SCAP mutant mice are therefore in terms with *in vitro* stud-

ies that report stimulation of synaptogenesis by addition of extracellular cholesterol (Camargo et al., 2012; Christopherson et al., 2005; Mauch et al., 2001; Nagler et al., 2001; Pfrieger, 2003b). Our studies are the first to show that astrocyte lipid metabolism is critical for proper synapse development *in vivo*.

#### 4.3 | SCAP mutants have affected vesicle populations at the presynapse

Hippocampal presynaptic terminals in SCAP mutants had a reduced number of synaptic vesicles that are ready for release, as well as a reduction in the total vesicle pool, therefore resulting in a smaller vesicle cluster size. This data and the observed impairment in synapse

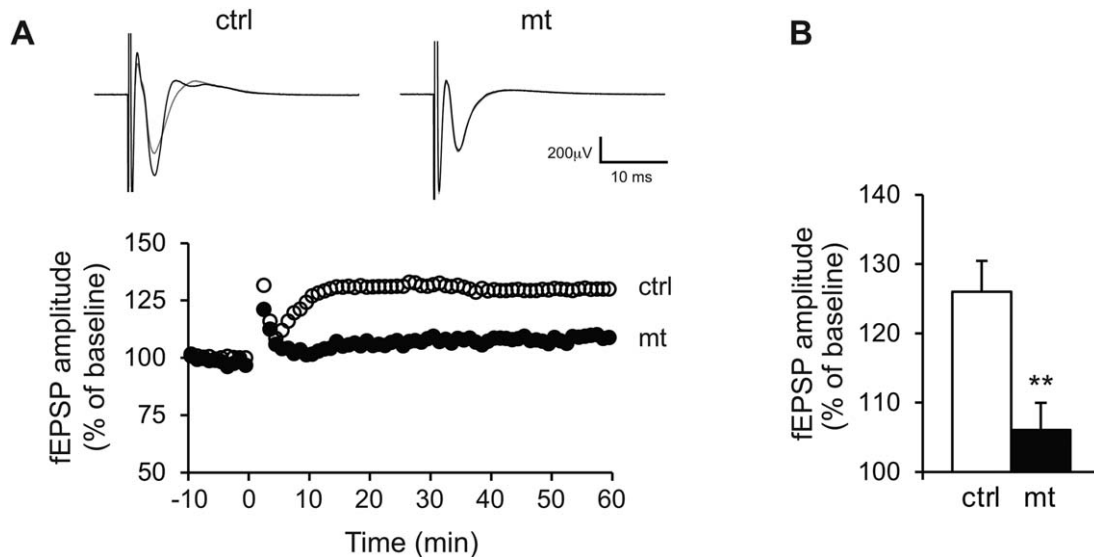


**FIGURE 7** Hippocampal LTP is impaired in SCAP mutants. (A) Upper panel: representative example of recorded potentials in hippocampal slices of control (ctrl) and mutant (mt) mice immediately after stimulation (gray line) and 20 min after stimulation (black line). Lower panel: representative example of LTP in a hippocampal slice of a control (open rounds) and a SCAP mutant mouse (filled rounds). (B) Histogram showing the average amplitude of fEPSP at 40–50 min after LTP induction recorded in slices of controls (white bar,  $n = 15$  slices) and mutants (black bar,  $n = 18$  slices). Data are presented as mean  $\pm$  SEM.  $**p < .01$ , Student's *t*-test

maturation in SCAP mutants, is consistent with published findings that immature synapses contain fewer synaptic vesicles (Mozhayeva, Sara, Liu, & Kavalali, 2002). Interestingly, also abnormal presynaptic protein expression was observed; significantly reduced SNAP-25 levels were found. SNAP-25 is a constituent of SNARE complexes and implicated in vesicle fusion (Jahn & Scheller, 2006; Rizo & Sudhof, 2002; Sollner et al., 1993; Sudhof & Rothman, 2009; Weber et al., 1998). Our finding that synapses of SCAP mutants contain reduced levels of the presynaptic protein SNAP-25 that is implicated in vesicle fusion is consistent with the observed reduced number of docked vesicles at the AZ. In contrast to the presynapse, we did not find any changes in postsynaptic protein level and ultrastructure in the hippocampus in SCAP mutants.

#### 4.4 | SCAP mutants have affected presynaptic function

In line with the observed abnormal proteins levels for SNAP-25 and vesicles number in presynaptic terminals, SCAP mutants were found impaired in PPF, suggesting that fewer synaptic vesicles were released in the presynaptic terminal leading to decreased neurotransmitter release. Our *in vivo* findings confirm the previously published *in vitro* studies that showed that cholesterol increased quantal content and enhanced synaptic efficacy (Christopherson et al., 2005; Clarke & Barres, 2013; Goritz, Mauch, Nagler, & Pfrieger, 2002; Mauch et al., 2001). Additionally, we show that astrocyte SCAP mutants have decreased LTP amplitude in the hippocampus. The observation that SCAP mutants have reduced number of synaptic vesicles in presynaptic terminals and impaired PPF, whereas no changes in postsynaptic terminal structure and protein levels were found, indicates that the presynaptic abnormalities may underlie the impaired LTP, a mechanism previously reported (Schulz, Cook, & Johnston, 1994).

Presynaptic terminals undergo extensive membrane remodelling during synaptic vesicle exocytosis and endocytosis, and several studies emphasized the role of lipids in this (Rituper, Flasker, Gucek, Chowdhury, & Zorec, 2012). The amount of cholesterol, as well as the length and saturation level of fatty acids, are important for the shape and flexibility of lipids, and thereby determine synaptic membrane thickness, curvature, and fluidity (Antonny, Vanni, Shindou, & Ferreira, 2015; Lauwers, Goodchild, & Verstreken, 2016). Accordingly, the synaptic vesicle cycle is sensitive to changes in lipid composition, for example, cholesterol binds synaptophysin, thereby affecting membrane curvature (Thiele et al., 2000). Cholesterol also increases synaptophysin binding to synaptobrevin leading to improved synaptic efficiency (Edelmann, Hanson, Chapman, & Jahn, 1995; Mitter et al., 2003). However, lowering of cholesterol levels has been shown to lead to a smaller vesicle pool (Lauwers et al., 2016; Rohrbough & Broadie, 2005) and impairs vesicle exocytosis through dispersion of clusters of plasma membrane-associated SNARE proteins, like SNAP-25 (Lang et al., 2001) for which we observed lower protein levels in synaptosomes. Palmitoylation appears to be the major targeting signal for SNAP-25 to associate with detergent resistant, cholesterol-enriched microdomains (Ammar, Kasas, Chasserot-Golaz, Bader, & Vitale, 2013). Remarkably, SNAP-25 is

one of the synaptic proteins with the highest metabolic turnover rate (Cohen et al., 2013), and alterations in SNAP-25 levels have been shown to cause impaired short-term synaptic plasticity (Johansson et al., 2008) and suggested to be implicated in paroxysmal dyskinesia (Lee et al., 2012; Nobile & Striano, 2014). Strikingly, these phenotypes are also observed for GFAP-SCAP mice (see Figure 6 and Camargo et al., 2012). How impaired astrocyte lipid metabolism underlies the observed reductions in SNAP-25 protein levels and presynaptic vesicle numbers in SCAP mutants remains to be determined. Taken together, these findings emphasize the importance of cholesterol and fatty acids in the synaptic vesicle cycle, and suggests that defective lipid supply by astrocytes of SCAP mutant mice is causal to the synaptic vesicle cycle leading to impaired presynaptic terminal development and function.

#### 4.5 | Implications for neurological disorders associated with defective astrocyte lipid metabolism

Several lipid metabolism disorders that are associated with synaptic dysfunction were found to have a compromised astrocyte metabolism. For instance, in HD, mutant huntingtin protein in astrocytes decreases SREBP maturation, leading to impaired cholesterol biosynthesis and secretion thereby affecting synapse numbers and activity (Valenza et al., 2015; Valenza et al., 2005). In addition, in the neurodegenerative disease NPC, mutations in the *NPC1* gene lead to impaired cholesterol transport in astrocytes (Patel et al., 1999), which may contribute to the impaired synaptic transmission (Xu et al., 2010). Finally, the lipid carrier apoE4, which is strongly expressed by astrocytes, is one of the most prevalent risk factors for AD (Poirier et al., 2014; Strittmatter et al., 1993), and deletion of apoE4 in mice causes reduced levels of cholesterol and its precursors in the hippocampus, which may contribute to the functional synaptic deficits found in AD (Levi et al., 2005; Zhong, Searce-Levie, Ramaswamy, & Weisgraber, 2008).

In summary, we found that a SCAP mutation in astrocytes resulted in impaired presynaptic terminal structure and function, possibly due to a reduced number of docked vesicles accompanied with small changes in presynaptic protein SNAP-25 expression. This study demonstrates an important role for astrocyte SCAP in brain lipid metabolism. Moreover it demonstrates the required contribution of lipid supply to adequate synaptic function *in vivo*, which improves our understanding of neurological disorders in which synaptic deficits have been associated with compromised brain lipid metabolism, such as in NPC, AD, and HD.

#### ACKNOWLEDGMENTS

We thank J. Wortel and R. Dekker for contribution to electron-microscopy preparations. We also thank H. Shimano for kindly providing SREBP antibodies and D. Gutmann for providing hGFAP-cre mice.

#### REFERENCES

- Abbott, L. F., & Regehr, W. G. (2004). Synaptic computation. *Nature*, 431, 796–803.



- Allen, J. A., Halverson-Tamboli, R. A., & Rasenick, M. M. (2007). Lipid raft microdomains and neurotransmitter signalling. *Nature Reviews Neuroscience*, 8, 128–140.
- Ammar, M. R., Kassas, N., Chasserot-Golaz, S., Bader, M. F., & Vitale, N. (2013). Lipids in Regulated Exocytosis: What are They Doing? *Frontiers in Endocrinology (Lausanne)*, 4, 125.
- An, J. J., Gharami, K., Liao, G. Y., Woo, N. H., Lau, A. G., Vanevski, F., ... Xu, B. (2008). Distinct role of long 3' UTR BDNF mRNA in spine morphology and synaptic plasticity in hippocampal neurons. *Cell*, 134, 175–187.
- Antonny, B., Vanni, S., Shindou, H., & Ferreira, T. (2015). From zero to six double bonds: phospholipid unsaturation and organelle function. *Trends in Cell Biology*, 25, 427–436.
- Arroyo-Olarte, R. D., Brouwers, J. F., Kuchipudi, A., Helms, J. B., Biswas, A., Dunay, I. R., ... Gupta, N. (2015). Phosphatidylthreonine and Lipid-Mediated Control of Parasite Virulence. *PLoS Biology*, 13, e1002288.
- Bajenaru, M. L., Zhu, Y., Hedrick, N. M., Donahoe, J., Parada, L. F., & Gutmann, D. H. (2002). Astrocyte-specific inactivation of the neurofibromatosis 1 gene (NF1) is insufficient for astrocytoma formation. *Molecular and Cellular Biology*, 22, 5100–5113.
- Boyles, J. K., Pitas, R. E., Wilson, E., Mahley, R. W., & Taylor, J. M. (1985). Apolipoprotein E associated with astrocytic glia of the central nervous system and with nonmyelinating glia of the peripheral nervous system. *Journal of Clinical Investigation*, 76, 1501–1513.
- Bu, G., Maksymovitch, E. A., Nerbonne, J. M., & Schwartz, A. L. (1994). Expression and function of the low density lipoprotein receptor-related protein (LRP) in mammalian central neurons. *Journal of Biological Chemistry*, 269, 18521–18528.
- Camargo, N., Brouwers, J. F., Loos, M., Gutmann, D. H., Smit, A. B., & Verheijen, M. H. (2012). High-fat diet ameliorates neurological deficits caused by defective astrocyte lipid metabolism. *FASEB Journal*, 26, 4302–4315.
- Camargo, N., Smit, A. B., & Verheijen, M. H. (2009). SREBPs: SREBP function in glia-neuron interactions. *FASEB Journal*, 23, 628–636.
- Chen, G., Li, H. M., Chen, Y. R., Gu, X. S., & Duan, S. (2007). Decreased estradiol release from astrocytes contributes to the neurodegeneration in a mouse model of Niemann-Pick disease type C. *Glia*, 55, 1509–1518.
- Chen, J., Zhang, X., Kusumo, H., Costa, L. G., & Guizzetti, M. (2013). Cholesterol efflux is differentially regulated in neurons and astrocytes: Implications for brain cholesterol homeostasis. *Biochimica et Biophysica Acta*, 1831, 263–275.
- Christopherson, K. S., Ullian, E. M., Stokes, C. C., Mallowney, C. E., Hell, J. W., Agah, A., ... Barres, B. A. (2005). Thrombospondins are astrocyte-secreted proteins that promote CNS synaptogenesis. *Cell*, 120, 421–433.
- Clarke, L. E., & Barres, B. A. (2013). Emerging roles of astrocytes in neural circuit development. *Nature Reviews Neuroscience*, 14, 311–321.
- Cohen, L. D., Zuchman, R., Sorokina, O., Muller, A., Dieterich, D. C., Armstrong, J. D., ... Ziv, N. E. (2013). Metabolic turnover of synaptic proteins: Kinetics, interdependencies and implications for synaptic maintenance. *PLoS One*, 8, e63191.
- Dietschy, J. M., & Turley, S. D. (2004). Thematic review series: Brain Lipids. Cholesterol metabolism in the central nervous system during early development and in the mature animal. *Journal of Lipid Research*, 45, 1375–1397.
- Eberle, D., Hegarty, B., Bossard, P., Ferre, P., & Foufelle, F. (2004). SREBP transcription factors: Master regulators of lipid homeostasis. *Biochimie*, 86, 839–848.
- Edelmann, L., Hanson, P. I., Chapman, E. R., & Jahn, R. (1995). Synaptobrevin binding to synaptophysin: A potential mechanism for controlling the exocytotic fusion machine. *EMBO Journal*, 14, 224–231.
- Goritz, C., Mauch, D. H., Nagler, K., & Pfrieger, F. W. (2002). Role of glia-derived cholesterol in synaptogenesis: New revelations in the synapse-glia affair. *Journal of Physiology-Paris*, 96, 257–263.
- Goritz, C., Thiebaut, R., Tessier, L. H., Nieweg, K., Moehle, C., Buard, I., ... Pfrieger, F. W. (2007). Glia-induced neuronal differentiation by transcriptional regulation. *Glia*, 55, 1108–1122.
- Harris, K. M., & Stevens, J. K. (1989). Dendritic spines of CA 1 pyramidal cells in the rat hippocampus: Serial electron microscopy with reference to their biophysical characteristics. *Journal of Neuroscience*, 9, 2982–2997.
- Hering, H., Lin, C. C., & Sheng, M. (2003). Lipid rafts in the maintenance of synapses, dendritic spines, and surface AMPA receptor stability. *Journal of Neuroscience*, 23, 3262–3271.
- Hua, X., Yokoyama, C., Wu, J., Briggs, M. R., Brown, M. S., Goldstein, J. L., & Wang, X. (1993). SREBP-2, a second basic-helix-loop-helix-leucine zipper protein that stimulates transcription by binding to a sterol regulatory element. *Proceedings of the National Academy of Sciences of the United States of America*, 90, 11603–11607.
- Jahn, R., & Scheller, R. H. (2006). SNAREs—engines for membrane fusion. *Nature Reviews Molecular Cellular Biology*, 7, 631–643.
- Jang, D. J., Park, S. W., & Kaang, B. K. (2009). The role of lipid binding for the targeting of synaptic proteins into synaptic vesicles. *BMB Reports*, 42, 1–5.
- Johansson, J. U., Ericsson, J., Janson, J., Beraki, S., Stanic, D., Mandic, S. A., ... Bark, C. (2008). An ancient duplication of exon 5 in the Snap25 gene is required for complex neuronal development/function. *PLoS Genetics*, 4, e1000278.
- Klychnikov, O. I., Li, K. W., Sidorov, I. A., Loos, M., Spijker, S., Broos, L. A., ... van den Maagdenberg, A. M. (2010). Quantitative cortical synapse proteomics of a transgenic migraine mouse model with mutated CaV2.1 calcium channels. *Proteomics*, 10, 2531–2535.
- Konur, S., Rabinowitz, D., Fenstermaker, V. L., & Yuste, R. (2003). Systematic regulation of spine sizes and densities in pyramidal neurons. *Journal of Neurobiology*, 56, 95–112.
- Kotti, T., Head, D. D., McKenna, C. E., & Russell, D. W. (2008). Biphasic requirement for geranylgeraniol in hippocampal long-term potentiation. *Proceedings of the National Academy of Sciences of the United States of America*, 105, 11394–11399.
- Ladner, C. L., Yang, J., Turner, R. J., & Edwards, R. A. (2004). Visible fluorescent detection of proteins in polyacrylamide gels without staining. *Analytical Biochemistry*, 326, 13–20.
- LaDu, M. J., Gilligan, S. M., Lukens, J. R., Cabana, V. G., Reardon, C. A., Van Eldik, L. J., & Holtzman, D. M. (1998). Nascent astrocyte particles differ from lipoproteins in CSF. *Journal of Neurochemistry*, 70, 2070–2081.
- Lang, T., Bruns, D., Wenzel, D., Riedel, D., Holroyd, P., Thiele, C., & Jahn, R. (2001). SNAREs are concentrated in cholesterol-dependent clusters that define docking and fusion sites for exocytosis. *EMBO Journal*, 20, 2202–2213.
- Lauwers, E., Goodchild, R., & Verstreken, P. (2016). Membrane Lipids in Presynaptic Function and Disease. *Neuron*, 90, 11–25.
- Lee, H. Y., Huang, Y., Bruneau, N., Roll, P., Roberson, E. D., Hermann, M., ... Ptáček, L. J. (2012). Mutations in the gene PRRT2 cause paroxysmal kinesigenic dyskinesia with infantile convulsions. *Cell Reports*, 1, 2–12.
- Levi, O., Lutjohann, D., Devir, A., von Bergmann, K., Hartmann, T., & Michaelson, D. M. (2005). Regulation of hippocampal cholesterol metabolism by apoE and environmental stimulation. *Journal of Neurochemistry*, 95, 987–997.
- Li, K. W., Miller, S., Klychnikov, O., Loos, M., Stahl-Zeng, J., Spijker, S., ... Smit, A. B. (2007). Quantitative proteomics and protein network

- analysis of hippocampal synapses of CaMKII $\alpha$  mutant mice. *Journal of Proteome Research*, 6, 3127–3133.
- Malatesta, P., Hack, M. A., Hartfuss, E., Kettenmann, H., Klinkert, W., Kirchhoff, F., & Gotz, M. (2003). Neuronal or glial progeny: Regional differences in radial glia fate. *Neuron*, 37, 751–764.
- Matsuda, M., Korn, B. S., Hammer, R. E., Moon, Y. A., Komuro, R., Horton, J. D., ... Shimomura, I. (2001). SREBP cleavage-activating protein (SCAP) is required for increased lipid synthesis in liver induced by cholesterol deprivation and insulin elevation. *Genes and Development*, 15, 1206–1216.
- Mauch, D. H., Nagler, K., Schumacher, S., Goritz, C., Muller, E. C., Otto, A., & Pfrieger, F. W. (2001). CNS synaptogenesis promoted by glia-derived cholesterol. *Science*, 294, 1354–1357.
- Medina, J. M., & Taberner, A. (2002). Astrocyte-synthesized oleic acid behaves as a neurotrophic factor for neurons. *The Journal of Physiology-Paris*, 96, 265–271.
- Meijer, M., Burkhardt, P., de Wit, H., Toonen, R. F., Fasshauer, D., & Verhage, M. (2012). Munc18-1 mutations that strongly impair SNARE-complex binding support normal synaptic transmission. *EMBO Journal*, 31, 2156–2168.
- Meng, Y., Zhang, Y., Tregoubov, V., Janus, C., Cruz, L., Jackson, M., ... Jia, Z. (2002). Abnormal spine morphology and enhanced LTP in LIMK-1 knockout mice. *Neuron*, 35, 121–133.
- Mitter, D., Reisinger, C., Hinz, B., Hollmann, S., Yelamanchili, S. V., Treiber-Held, S., ... Ahnert-Hilger, G. (2003). The synaptophysin/synaptobrevin interaction critically depends on the cholesterol content. *Journal of Neurochemistry*, 84, 35–42.
- Mozhayeva, M. G., Sara, Y., Liu, X., & Kavalali, E. T. (2002). Development of vesicle pools during maturation of hippocampal synapses. *Journal of Neuroscience*, 22, 654–665.
- Nagler, K., Mauch, D. H., & Pfrieger, F. W. (2001). Glia-derived signals induce synapse formation in neurones of the rat central nervous system. *Journal of Physiology*, 533, 665–679.
- Nieweg, K., Schaller, H., & Pfrieger, F. W. (2009). Marked differences in cholesterol synthesis between neurons and glial cells from postnatal rats. *Journal of Neurochemistry*, 109, 125–134.
- Nobile, C., & Striano, P. (2014). PRRT2: A major cause of infantile epilepsy and other paroxysmal disorders of childhood. *Progress in Brain Research*, 213, 141–158.
- Patel, S. C., Suresh, S., Kumar, U., Hu, C. Y., Cooney, A., Blanchette-Mackie, E. J., ... Ong, W. Y. (1999). Localization of Niemann-Pick C1 protein in astrocytes: implications for neuronal degeneration in Niemann-Pick type C disease. *Proceedings of the National Academy of Sciences of the United States of America*, 96, 1657–1662.
- Pfrieger, F. W. (2003a). Cholesterol homeostasis and function in neurons of the central nervous system. *Cellular and Molecular Life Sciences*, 60, 1158–1171.
- Pfrieger, F. W. (2003b). Role of cholesterol in synapse formation and function. *Biochimica et Biophysica Acta*, 1610, 271–280.
- Pfrieger, F. W., & Ungerer, N. (2011). Cholesterol metabolism in neurons and astrocytes. *Progress in Lipid Research*, 50, 357–371.
- Piomelli, D., Astarita, G., & Rapaka, R. (2007). A neuroscientist's guide to lipidomics. *Nature Reviews Neuroscience*, 8, 743–754.
- Poirier, J., Miron, J., Picard, C., Gormley, P., Theroux, L., Breitner, J., & Dea, D. (2014). Apolipoprotein E and lipid homeostasis in the etiology and treatment of sporadic Alzheimer's disease. *Neurobiology of Aging*, 35, S3–10.
- Rituper, B., Flasker, A., Gucek, A., Chowdhury, H. H., & Zorec, R. (2012). Cholesterol and regulated exocytosis: A requirement for unitary exocytotic events. *Cell Calcium*, 52, 250–258.
- Rizo, J., & Sudhof, T. C. (2002). Snares and Munc18 in synaptic vesicle fusion. *Nature Reviews Neuroscience*, 3, 641–653.
- Rohrbough, J., & Broadie, K. (2005). Lipid regulation of the synaptic vesicle cycle. *Nature Reviews Neuroscience*, 6, 139–150.
- Schulz, P. E., Cook, E. P., & Johnston, D. (1994). Changes in paired-pulse facilitation suggest presynaptic involvement in long-term potentiation. *Journal of Neuroscience*, 14, 5325–5337.
- Semple, B. D., Blomgren, K., Gimlin, K., Ferriero, D. M., & Noble-Haeusslein, L. J. (2013). Brain development in rodents and humans: Identifying benchmarks of maturation and vulnerability to injury across species. *Progress in Neurobiology*, 106–107, 1–16.
- Sollner, T., Whiteheart, S. W., Brunner, M., Erdjument-Bromage, H., Gorman, S., Tempst, P., & Rothman, J. E. (1993). SNAP receptors implicated in vesicle targeting and fusion. *Nature*, 362, 318–324.
- Spell, C., Kolsch, H., Lutjohann, D., Kerksiek, A., Hentschel, F., Damian, M., ... Heun, R. (2004). SREBP-1a polymorphism influences the risk of Alzheimer's disease in carriers of the ApoE4 allele. *Dementia and Geriatric Cognitive Disorders*, 18, 245–249.
- Strittmatter, W. J., Saunders, A. M., Schmechel, D., Pericak-Vance, M., Enghild, J., Salvesen, G. S., & Roses, A. D. (1993). Apolipoprotein E: High-avidity binding to beta-amyloid and increased frequency of type 4 allele in late-onset familial Alzheimer disease. *Proceedings of the National Academy of Sciences of the United States of America*, 90, 1977–1981.
- Sudhof, T. C., & Rothman, J. E. (2009). Membrane fusion: Grappling with SNARE and SM proteins. *Science*, 323, 474–477.
- Thiele, C., Hannah, M. J., Fahrenholz, F., & Huttner, W. B. (2000). Cholesterol binds to synaptophysin and is required for biogenesis of synaptic vesicles. *Nature Cell Biology*, 2, 42–49.
- Toni, N., Teng, E. M., Bushong, E. A., Aimone, J. B., Zhao, C., Consiglio, A., ... Gage, F. H. (2007). Synapse formation on neurons born in the adult hippocampus. *Nature Neuroscience*, 10, 727–734.
- Valenza, M., Marullo, M., Di Paolo, E., Cesana, E., Zuccato, C., Biella, G., & Cattaneo, E. (2015). Disruption of astrocyte-neuron cholesterol cross talk affects neuronal function in Huntington's disease. *Cell Death & Differentiation*, 22, 690–702.
- Valenza, M., Rigamonti, D., Goffredo, D., Zuccato, C., Fenu, S., Jamot, L., ... Cattaneo, E. (2005). Dysfunction of the cholesterol biosynthetic pathway in Huntington's disease. *Journal of Neuroscience*, 25, 9932–9939.
- Verheijen, M. H., Camargo, N., Verdier, V., Nadra, K., de Preux Charles, A.S., Medard, J. J., ... Smit, A. B. (2009). SCAP is required for timely and proper myelin membrane synthesis. *Proceedings of the National Academy of Sciences of the United States of America*, 106, 21383–21388.
- Waterham, H. R., Wijburg, F. A., Hennekam, R. C., Vreken, P., Poll-The, B. T., Dorland, L., ... Wanders, R. J. (1998). Smith-Lemli-Opitz syndrome is caused by mutations in the 7-dehydrocholesterol reductase gene. *American Journal of Human Genetics*, 63, 329–338.
- Weber, T., Zemelman, B. V., McNew, J. A., Westermann, B., Gmachl, M., Parlato, F., ... Rothman, J. E. (1998). SNAREpins: minimal machinery for membrane fusion. *Cell*, 92, 759–772.
- Worgall, T. S. (2011). Sphingolipid synthetic pathways are major regulators of lipid homeostasis. *Advances in Experimental Medicine and Biology*, 721, 139–148.
- Xu, S., Zhou, S., Xia, D., Xia, J., Chen, G., Duan, S., & Luo, J. (2010). Defects of synaptic vesicle turnover at excitatory and inhibitory synapses in Niemann-Pick C1-deficient neurons. *Neuroscience*, 167:608–620.
- Yokoyama, C., Wang, X., Briggs, M. R., Admon, A., Wu, J., Hua, X., ... Brown, M. S. (1993). SREBP-1, a basic-helix-loop-helix-leucine zipper



protein that controls transcription of the low density lipoprotein receptor gene. *Cell*, 75, 187–197.

Yuste, R., & Bonhoeffer, T. (2004). Genesis of dendritic spines: Insights from ultrastructural and imaging studies. *Nature Reviews Neuroscience*, 5, 24–34.

Zhong, N., Scearce-Levie, K., Ramaswamy, G., & Weisgraber, K. H. (2008). Apolipoprotein E4 domain interaction: Synaptic and cognitive deficits in mice. *Alzheimer's & Dementia*, 4, 179–192.

Zhuo, L., Theis, M., Alvarez-Maya, I., Brenner, M., Willecke, K., & Messing, A. (2001). hGFAP-cre transgenic mice for manipulation of glial and neuronal function in vivo. *Genesis*, 31, 85–94.

## SUPPORTING INFORMATION

Additional Supporting Information may be found in the online version of this article.

**How to cite this article:** van Deijk A-LF, Camargo N, Timmerman J, et al. Astrocyte lipid metabolism is critical for synapse development and function in vivo. *Glia*. 2017;00:1–13. <https://doi.org/10.1002/glia.23120>